



RESEARCH LETTER

10.1029/2018GL079099

Key Points:

- We find high ion upflow occurrence near MLAT $\sim 78^\circ$ and associated with particle precipitation (high T_e , low T_i/T_e , high FAC)
- The ion upflow flux increases with increased FAC and convection speed. When T_i/T_e ratio increases, the upflow occurrence and flux decreases
- The average vertical flow turns upward when $T_i/T_e < 0.8$ or $T_e > T_i + 600$ K

Supporting Information:

- Supporting Information S1

Correspondence to:

Q.-H. Zhang,
zhangqinghe@sdu.edu.cn

Citation:

Ma, Y.-Z., Zhang, Q.-H., Xing, Z.-Y., Heelis, R. A., Oksavik, K., & Wang, Y. (2018). The ion/electron temperature characteristics of polar cap classical and hot patches and their influence on ion upflow. *Geophysical Research Letters*, 45. <https://doi.org/10.1029/2018GL079099>

Received 6 JUN 2018

Accepted 13 AUG 2018

Accepted article online 23 AUG 2018

The Ion/Electron Temperature Characteristics of Polar Cap Classical and Hot Patches and Their Influence on Ion Upflow

Yu-Zhang Ma¹, Qing-He Zhang¹ , Zan-Yang Xing¹ , Roderick A. Heelis² , Kjellmar Oksavik^{3,4} , and Yong Wang¹ 

¹Shandong Provincial Key Laboratory of Optical Astronomy and Solar-Terrestrial Environment, Institute of Space Sciences, Shandong University, Weihai, China, ²William B. Hanson Center for Space Sciences, University of Texas at Dallas, Richardson, TX, USA, ³Birkeland Centre for Space Science, University of Bergen, Bergen, Norway, ⁴Arctic Geophysics, University Centre in Svalbard, Longyearbyen, Norway

Abstract The term of “polar cap hot patch” is a newly identified high-density plasma irregularity at high latitudes, which is associated with high electron temperature and particle precipitation, while a classical polar cap patch has lower electron temperature. To investigate characteristics of hot patches versus classical patches, five years of in situ database of plasma observations from the DMSP satellites was analyzed. For the first time, we show how the ion/electron temperature ratio (or temperature difference) can be used to distinguish between classical and hot patches. For classical patches ($T_i/T_e > 0.8$ or $T_e < T_i + 600$ K), the vertical ion flux is generally downward. For hot patches ($T_i/T_e < 0.8$ or $T_e > T_i + 600$ K), the vertical ion flux is generally upward. The highest upflow occurrence was found near the polar cap boundary, associated with hot patches, particle precipitation, strong convection speed, and localized field-aligned currents. This result shows that the polar cap hot patches may play a very important role in solar wind-magnetosphere-ionosphere coupling processes.

Plain Language Summary The polar ionosphere is one of the most dynamical regions on Earth, where energy, mass, and momentum can flow between the solar wind and the upper atmosphere. One important phenomenon in the polar ionosphere is polar cap patches, which are islands of high-density plasma. The polar cap patches are often associated with sharp density gradients that cause disturbances to radio signals, satellite navigation, and communication. A new type of patch, associated with strong scintillation, has recently been identified in literature and called “polar cap hot patch.” In this paper we compare the plasma characteristics of “classical” and “hot” patches. For the first time, we show how the ion/electron temperature ratio (or temperature difference) can be used to distinguish between classical and hot patches. We find high ion upflow occurrence associated with particle precipitation in the hot patches. The ion upflow flux increases with increased field-aligned current and convection speed. This shows that the polar cap hot patches may play a very important role in solar wind-magnetosphere-ionosphere coupling processes.

1. Introduction

The polar ionosphere is one of the most dynamical regions on Earth, where energy, mass, and momentum can flow between the solar wind and the upper atmosphere. One important phenomenon generated by the solar wind-magnetosphere-ionosphere coupling is polar cap patches, which are defined as islands of high-density ionospheric plasma in the *F* region. Patches are often thought to be generated by ionospheric cusp dynamics during southward interplanetary magnetic field (IMF) conditions (e.g., Crowley, 1996). The typical size of a patch is around 100 to 1,000 km (Coley & Heelis, 1995), the plasma density is twice that of the surrounding region (e.g., Crowley, 1996), and the electron temperature is often comparable to or lower than the ion temperature. After formation near the cusp, the patch transits the polar cap along the convection streamlines from the dayside to the nightside, where it exits the polar cap and is transported into the nightside auroral oval (e.g., Zhang, Zhang, Moen, et al., 2013; Zhang et al., 2015). In literature the properties of patches have been investigated using all-sky airglow imagers (Weber et al., 1984), GPS total electron content data (Foster et al., 2005), or incoherent scatter radar (Carlson et al., 2002; Lockwood et al., 2005; Zhang

et al., 2011). Some processes that have been proposed for generation of patches are the following: continuous tongues of plasma that are cut into segments by plasma flow jet channels (Valladares et al., 1998); IMF reversals and plasma production by cusp particle precipitation (Millward et al., 1999; Rodger et al., 1994); and transient magnetopause reconnection, causing equatorward excursion of the open-closed boundary and high-density solar EUV ionized plasma from lower latitudes transported into the polar cap (Carlson Jr et al., 2004; Foster et al., 2005; Lockwood & Carlson, 1992; Lockwood et al., 2005; Zhang et al., 2011; Zhang, Zhang, Lockwood, et al., 2013). Ionization due to particle precipitation has also been suggested as a source of polar cap patches (MacDougall & Jayachandran, 2007; Oksavik et al., 2006; Weber et al., 1984). This type of patch is often associated with poleward moving auroral forms. However, poleward moving auroral forms are optical auroral structures generated by particle precipitation due to newly opened flux tubes (by dayside magnetopause reconnection) that move poleward and are not always associated with islands of high-density plasma (i.e., 10^5 cm^{-3}) in the F region (e.g., Carlson, 2012; Zhang et al., 2013). There can also be patches that are not associated with poleward moving auroral forms (e.g., Oksavik et al., 2015). Zou et al. (2015, 2016, 2017) have published a series of papers on airglow patches by combining in situ and ground-based observations. They found that some of airglow patches are associated with enhanced polar cap flow, strong localized field-aligned currents, and low-energy precipitation. For large negative IMF B_y , the airglow patch near the polar cap boundary can be associated with very fast antisunward flow ($> \sim 1,500 \text{ m/s}$; Wang et al., 2016). Recently, Zhang et al. (2017) used DMSP F16 in situ measurements to identify a similar enhanced density structure (electron density $6.6 \times 10^5 \text{ cm}^{-3}$ at 860-km altitude) in the topside F region polar cap. They called it a “polar cap hot patch,” which has similar electron density to classical patches ($5.5 \times 10^5 \text{ cm}^{-3}$), but has much higher electron temperature (3,800 K for hot patches versus 2,200 K for classical patches at 860-km altitude). Zhang et al. (2017) suggested that the hot patches may be produced when flow channels transport photoionization plasma through and area of low-energy particle precipitation, localized field-aligned currents, and are those associated with ion upflows. These observations suggest that hot patches may be the initial creation phase of classical patches, and the classical (cold) patches are more mature patches that with temperature have cooled down as the particle precipitation has ended during their transpolar evolution.

Significant ion upflow can be generated if the enhanced plasma density of a “classical” polar cap patch is accompanied by enhanced antisunward convection (Zhang et al., 2016) or a “hot” polar cap patch is associated with particle precipitation and strong field-aligned currents (Zhang et al., 2017). However, the ion and electron temperature in these two situations are totally different; the electron temperature is much higher than the ion temperature for the hot versus the classical patches. The acceleration mechanisms for upwelling ions are generally associated with the electron and ion temperatures in the following two principal ways: (a) the electromagnetic energy flow (i.e., the Poynting flux) can heat ions in the E and lower F regions giving enhanced ion temperatures and (b) the particle energy flow (i.e., soft electron precipitation) giving enhanced electron temperatures. The Poynting flux results in ion frictional heating or various current-driven waves and instabilities, thereby increasing the scale height and the ion temperature. The electron precipitation modifies the electron temperature and density in the F region ionosphere, resulting in ion upwelling through the ambipolar electric field associated with the enhanced electron temperature (Strangeway et al., 2005). Sometimes electron and ion heating may both be active in the same regions (Skjæveland et al., 2011, 2014). Thus, the ion/electron temperature ratio may be a good way to separate classical from hot patches and in addition provide information on how the associated ion upflows are generated.

In this study, we have identified more than 3,000 patches in DMSP F16 and F17 data for the period of 2010–2014. We analyze the in situ plasma features inside these patches and discuss the influence of the temperature and the ion/electron temperature ratio on ion upflows.

2. Data and Methods

2.1. Data Set

DMSP satellites are in a Sun-synchronous polar orbit at an altitude of 830 km. Each satellite has an orbital period of approximately 101 min. The SSJ/4 detectors onboard the DMSP satellites obtain the differential energy flux of the electrons and ions from 32 eV to 30 keV. In this study we also use the ion and oxygen density (Ni and N_O^+), the ion horizontal cross-track velocity (V_y , positive in the sunward direction), the ion vertical velocity

(V_z , positive in the upward direction), and the ion and electron temperatures (T_i and T_e) from the SSIES instrument. The time resolution is 1 s, and the data are used to calculate the vertical flux of O^+ via the product $N_{O^+} \cdot V_z$. The magnetic field data from the SSM instrument have 1-s time resolution, and it is used to estimate the field-aligned current via dB/dt .

2.2. Identification of a Polar Cap Patch

By using the method of Ma et al. (2018), the polar cap boundaries can be identified for each DMSP pass by locating the high-energy electron precipitation cutoff and the convection reversal. Next we estimate the average plasma density across the polar cap, and use it as the level of the background plasma density. Next we find the locations where the plasma density is more than 2 times higher than this background. The horizontal extent of a patch should exceed 20 s (corresponding to a minimum size of about 140 km for a satellite velocity of around 7 km/s).

3. Observations and Results

3.1. Case Study on 4 November 2014, 19:52–20:12 UT

A typical example of a polar cap transit is given in Figure 1. From top to bottom, the parameters shown are (a) total ion and O^+ density, (b) ion cross-track velocity and vertical velocity, (c) vertical flux (oxygen density multiplied by the vertical velocity), (d) ion and electron temperature (T_i and T_e), (e) field-aligned current, and (f and g) electron and ion differential precipitation energy flux. The polar cap boundary is marked by the black dashed lines, and polar cap patches A and B are highlighted by the red dashed line and the gray shading. The O^+ number densities of patch A and patch B are both around $8.0 \times 10^4 \text{ cm}^{-3}$. However, their motion and plasma temperature are different: the cross-track velocity of patch A reaches $-1,000 \text{ m/s}$ while that of patch B is only -200 m/s . The electron temperature in patch A is 4,000 K and much higher than the ion temperature (around 2,000 K). In patch B, however, the electron temperature is similar to the ion temperature (around 2,500 K). In Figure 1e, the upward current is observed in patch A but is essentially absent in patch B. Soft electron precipitation is associated with patch A (Figure 1f), which is suggestive of electron heating through soft electron precipitation. This also explains the upward flux in patch A. Patches near the polar cap boundary like patch A are termed polar cap hot patches, which are accompanied by strong electron precipitation, localized field-aligned currents, and ion upflows (Zhang et al., 2017). For such patches the electron temperature is much higher than the ion temperature. For classical polar cap patches like patch B, the vertical flux is downward and the electron temperature decreases to the same level as the ion temperature. In the next section we look at how the difference between the electron and ion temperatures influences the ion upflow occurrence.

3.2. Statistical Study

By using five years (2010–2014) of plasma observations from the Northern Hemisphere for DMSP F16 and F17, we found 3,565 patches. The magnetic local time (MLT)/magnetic latitude (MLAT) distributions of plasma parameters for these patches are shown in Figure 2. In order to obtain a wider data coverage, we have combined data from both F16 and F17 in this study. Although artificial biases might appear due to the mixing of data from different satellites with different orbital planes and data baselines, the overall distribution of plasma parameters remains very similar for each satellite (not shown) and the conclusions should not be affected. The patches occur more frequently around 80° MLAT, 15–18 MLT than in the prenoon sector (Figure 2a). In the noon sector or the central polar cap, the convection speed is lower than in the dawn/dusk region (before 9 and after 17 MLT) around 80° MLAT (Figure 2b). After comparing the averaged IMF and convection speed data for each patch (Figures S2 and S3), and consistent with Wang et al. (2016), the patch occurrence rate is higher near the polar cap boundary (around 80° MLAT) where there is larger convection speed for strongly negative IMF B_y . The field-aligned current is higher near 80° MLAT than in the central polar cap ($>85^\circ$ MLAT), and it is downward in the postnoon sector and upward in the prenoon sector (Figure 2c), which may be associated with the region 0 cusp current system (Iijima & Potemra, 1976). The current distribution is wide in MLT and MLAT, which may be caused by our averaging of different IMF B_y conditions. The electron temperature is about 2,000–2,500 K in the noon sector of the central polar cap ($>85^\circ$ MLAT), and it is highest in the dusk sector between 75 and 80° MLAT ($>3,000 \text{ K}$; Figure 2d). The ion temperature is highest in the noon sector of the central polar cap ($>85^\circ$ MLAT) and in the dusk sector around 75° MLAT ($>2,400 \text{ K}$; Figure 2e). Therefore, the T_i/T_e ratio is also highest near noon in the central polar cap

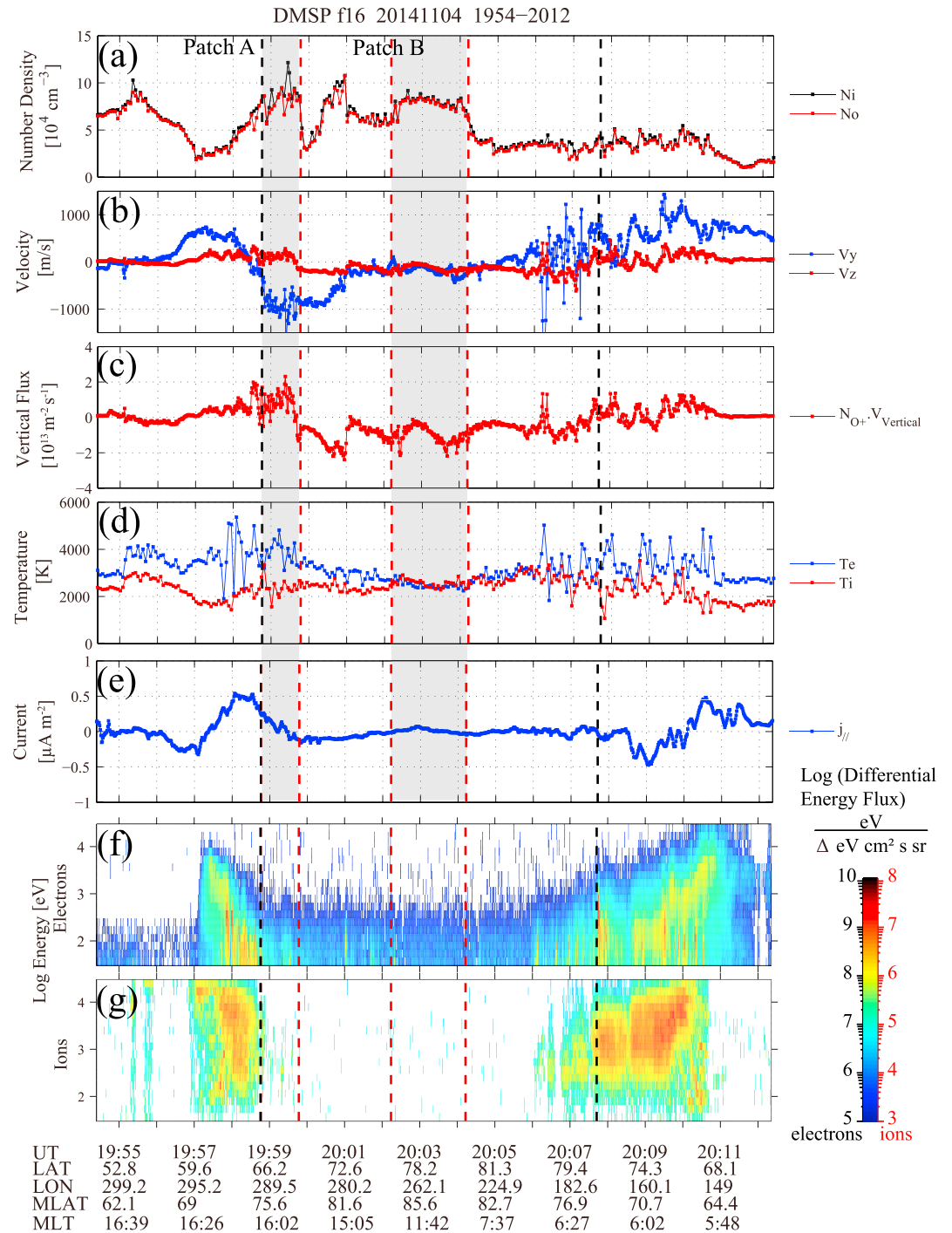


Figure 1. Typical DMSP F16 data from a transit of the polar cap on 4 November 2014 at 19:54–20:12 UT. The polar cap is marked with black dashed lines, and two polar cap patches (a and b) are marked with red dashed lines and gray shading inside. From top to bottom, the panels show (a) the ion and O^+ density, (b) the cross-track velocity (V_y) and the vertical velocity (V_z), (c) the vertical flux, (d) the electron and ion temperatures, (e) the field-aligned current, (f) the electron energy flux, and (g) the ion energy flux.

region ($>85^\circ$ MLAT; Figure 2f). The oxygen density is highest in the noon and postnoon sectors (Figure 2g). The vertical velocity in our paper is positive for upflow. The ion upflow occurrence and flux are highest around 80° MLAT (Figures 2h and 2i), and encompass the regions of low T_i/T_e region and high convection

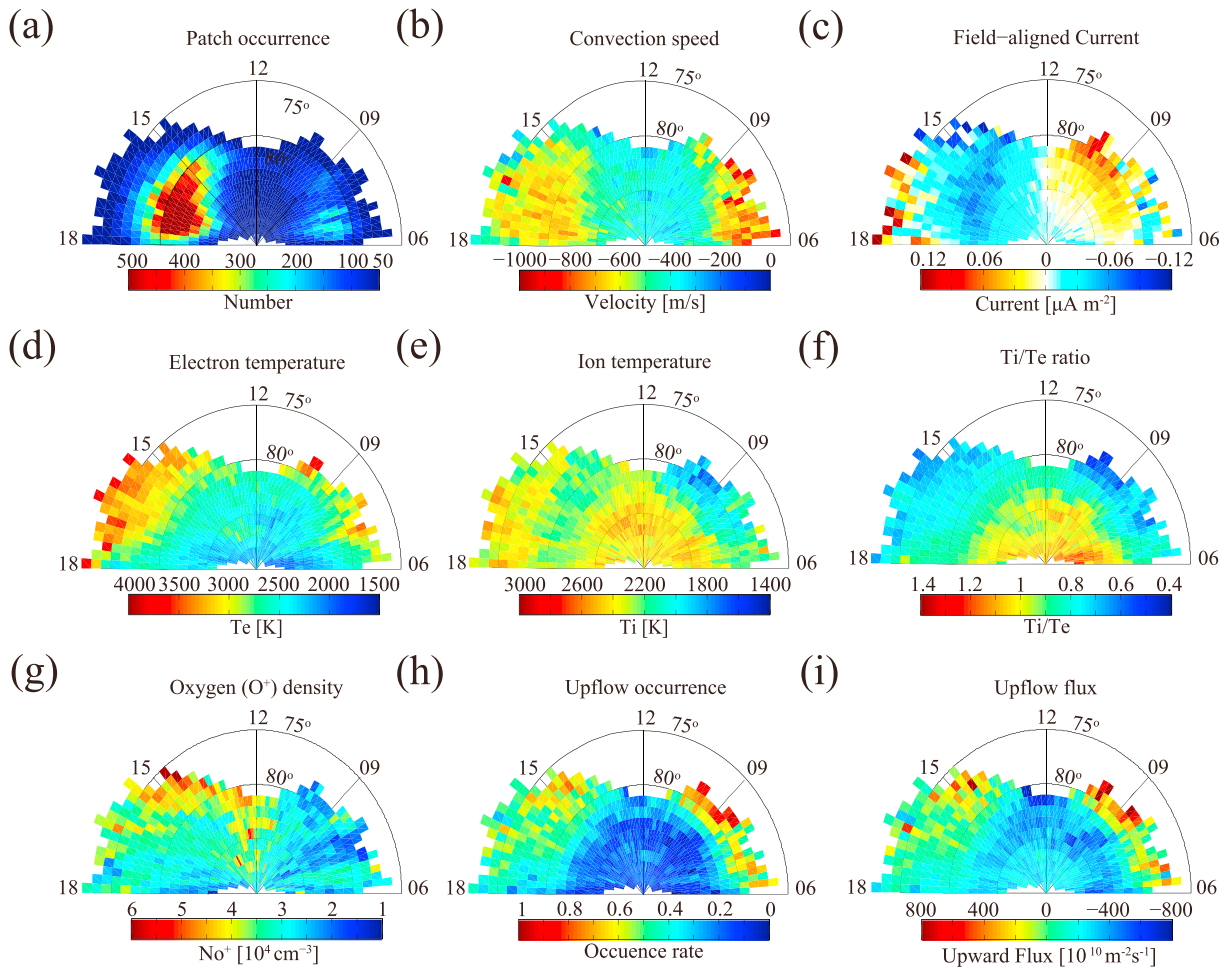


Figure 2. MLAT-MLT distribution of (a) patch occurrence, (b) convection speed, (c) field-aligned current, (d) electron temperature (T_e), (e) ion temperature (T_i), (f) the T_i/T_e ratio, (g) the O^+ density, (h) upflow occurrence, and (i) upflow flux. The distributions are averaged in bins over 1° MLAT and 12 min MLT. Only data bins having more than 20 samples are plotted.

speed. In the central polar cap, where the T_i/T_e is larger and the convection speeds are smaller, the upflow occurrence decreases to less than 0.2, and the flux turns downward.

In Figure 3, we show the ion upflow flux versus convection speed and field-aligned current for different T_i/T_e ratios (from 0.4–0.6 to 1.4–1.6). In Figures 3a–3f, for convection speeds less than about 800 m/s, the ion upflow is weak or downward unless the electron temperature significantly exceeds the ion temperature in regions of localized field-aligned current and precipitation. As the convection speed increases, upflows may be seen when the electron temperature is not elevated above the ion temperature. These observations were assigned to frictional heating described previously by Zhang et al. (2016), which only occur when the plasma convection speed exceeds 1,000 m/s. Many more upflow events associated with plasma patches occur when the electron temperature exceeds the ion temperature. In these cases the upflow flux is strongly dependent on the localized field-aligned current intensity and more weakly dependent on the convective flow.

Figure 3g summarizes the influence of the T_i/T_e ratio on the upflow occurrence and flux. Each point presents an average at each temperature ratio. T_i , T_e , and the upflow flux are shown in red, blue, and green, respectively. The shading indicates the error bars. When the T_i/T_e ratio increases from 0.4 to 1.6, the electron temperature decreases from $\sim 3,600$ to $\sim 2,000$ K, and the ion temperature increases from $\sim 1,500$ to $\sim 3,000$ K. The corresponding upflow occurrence shown by the black line decreases from 0.8 to less than 0.1, and the vertical flux turns downward at $T_i/T_e = 0.8$ ($T_e = T_i + 600$ K; Figure S1).

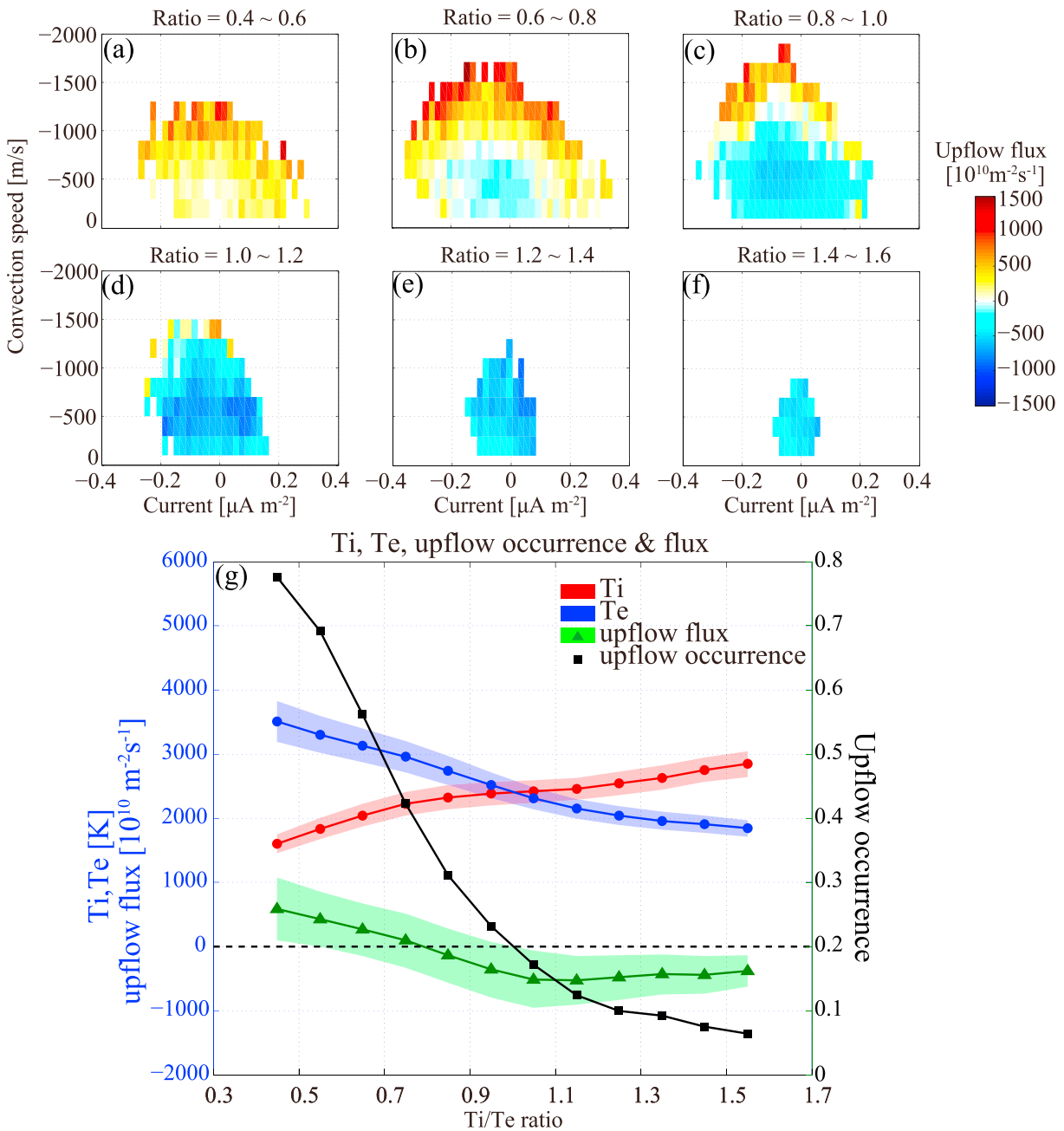


Figure 3. (a–f) Ion upflow flux versus convection speed and field-aligned current for different T_i/T_e ratios. The distributions are averaged in bins over 200 m/s and 0.02 μA . (g) Ion upflow flux (green), electron temperature (blue), ion temperature (red), and upflow occurrence (black) versus the T_i/T_e ratio.

4. Discussion

In Figure 2, we found that the ion temperature is almost as large as the electron temperature ($T_i/T_e > 0.9$) in the central polar cap, where the field-aligned current is small. These parameters suggest that the patches in the central polar cap are the so-called “classical patches”, which are formed by high-density plasma that transits through the cusp region from lower latitudes. Patches around 75° MLAT are associated with significant field-aligned current, strong convection speed, and higher electron temperature ($T_i/T_e < 0.8$) and appear to be the polar cap hot patches (Zhang et al., 2017). The upflow occurrence is higher in the hot patches, possibly due to the electron precipitation which moves ions upward through the ambipolar electric field (Strangeway et al., 2005) with additional contributions from frictional heating associated with strong convection speed

(Figure 2b; around 800 m/s antisunward) associated with frictional heating (Zhang et al., 2016). Compared to the hot patches that have high convection speed and strong field-aligned current, the classical patches in the central polar cap generally show lower convection speed, weaker current, and lower electron temperature compared to the ion temperature. Consequently, the classical patches normally have a lower upflow occurrence (<0.2). These statistical results confirm that hot patches are the initial creation phase of patches and associated with particle precipitation and bursty plasma flow. The classical (cold) patches are more mature patches where the particle precipitation has ended and the convection speed is low.

The presence of particle precipitation affects the ionization rate and energy flux, which influence the electron temperature and upward ion flux. This is evident in Figures 3a–3f, where the upward flux is dependent on the field-aligned current density. In the absence of significant localized field-aligned currents, the upward flux is also dependent on both the ion/electron temperature ratio and the convection speed. As the T_i/T_e ratio increases, a higher convection speed is needed to turn the flux upward, suggesting that ions need more frictional heating at a lower electron temperature to move upward. Ma et al. (2018) suggest that the convection speed may influence the upflow over the polar cap in two ways: frictional heating or the time history of the field line. Strong particle precipitation in the cusp region will heat the local ionosphere and produce ion upflow. The latitudinal extent of the “cusp fountain” (Horwitz & Lockwood, 1985), produced by strong convective flows and particle heating, is dependent on the flow speed. With time some of these upflowing ions will fall back down due to gravity. For a larger convection speed, it will take less time for the field line to move, and the upflow will persist and be observed by a satellite in the polar cap. For a lower convection speed, it will take more time to move the field line, and the satellite will instead observe ions that move downward. One can also look at the temperature difference (Figure S1). It shows a similar distribution to the T_i/T_e ratio, where the upward flux is obvious when $T_e > T_i + 600$ K, and the vertical flux increases with increasing field-aligned current and convection speed. It seems that the vertical flux in patches is more likely upward when the electron temperature is higher. In other words, the hot patches with higher electron temperature could be a more important upflow source than classical patches. Note that the polar cap temperature also depends on the solar zenith angle (SZA; e.g., Kitamura et al., 2011). However, the average SZA varies only by around 6° as the MLAT increases from 75° to 88° . In our statistical study there is only an $\sim 5^\circ$ SZA variation in a single satellite pass due to the dusk-dawn orbit (Ma et al., 2018), suggesting that the observed temperature enhancement is mainly due to particle precipitation rather than SZA effects.

Figure 3g shows that the vertical flux has a clear dependence on the electron temperature or specifically the T_i/T_e ratio. $T_i/T_e = 0.8$ ($T_e = T_i + 600$ K), seems to be a threshold value for the reversal of the flux, at least at the altitude of the DMSP spacecraft (around 860 km). It can be used to distinguish hot patches from classical patches. However, a hot patch may make a transition to a classic patch if it is observed outside the precipitation region where the electron temperature has cooled but the electron density remains high. Thus, the identification should also be verified with electron precipitation or other parameters.

5. Conclusion

By analyzing a five-year period of DMSP observations, we investigated the ion and electron temperature influence on the upflow in polar cap patches and hot patches. Patches were more frequent on the duskside of the polar cap. Patches in the central polar cap had lower convection speed, lower localized field-aligned current, and higher T_i/T_e ratio than patches near the polar cap boundary. We suggest that patches in the central polar cap belong to the category of “classical patch,” while the others are the “hot patches.” Higher upflow occurrence is observed in hot patches due to the electron precipitation giving enhanced electron temperature and lower T_i/T_e ratio.

The variation of the T_i/T_e ratio (or $T_e - T_i$ difference) influences the ion upflow in the classical patches and hot patches. As the T_i/T_e ratio or the $T_e - T_i$ difference increases, which implies that the patches are turning from hot patches to classical patches, the vertical flux turns from upward to downward. The vertical flux also increases with the increasing convection speed, which corresponds to frictional heating and patch evolution (Ma et al., 2018; Zhang et al., 2016) and localized field-aligned current associated with electron heating (Strangeway et al., 2005). When $T_i/T_e = 0.8$, or $T_e = T_i + 600$ K, we see a transition between upward and downward flux in the DMSP data set. We therefore propose to use this criterion to separate between classical and hot polar cap patches.

Acknowledgments

This work was supported by the National Natural Science Foundation of China (grants 41574138, 41604139, 41431072, and 41774166), the Young Top-Notch Talent Program of the "National High-level Personnel of Special Support Program (Ten Thousand Talent Program)," the Chinese Meridian Project, and the Shandong Provincial Natural Science Foundation (grant JQ201412). K.O. was supported by funding from the Research Council of Norway grant 223252. We thank the NOAA FTP and JHU/APL for making available the DMSP data (<https://satdat.ngdc.noaa.gov/dmsp/data/>). The authors also thank the International Space Science Institute in Beijing (ISSI-BJ) for supporting and hosting the meetings of the International Team on "Multiple instrument observations and simulations of the dynamical processes associated with polar cap patches/aurora and their associated scintillations," during which the discussions leading/contributing to this publication were held.

References

- Carlson, H. C. (2012). Sharpening our thinking about polar cap ionospheric patch morphology, research, and mitigation techniques. *Radio Science*, *47*, RS0L21. <https://doi.org/10.1029/2011RS004946>
- Carlson, H. C., Oksavik, K., Moen, J., van Eyken, A. P., & Guio, P. (2002). ESR mapping of polar-cap patches in the dark cusp. *Geophysical Research Letters*, *29*(10), 1386. <https://doi.org/10.1029/2001GL014087>
- Carlson, H. C. Jr., Oksavik, K., Moen, J., & Pedersen, T. (2004). Ionospheric patch formation: Direct measurements of the origin of a polar cap patch. *Geophysical Research Letters*, *31*, L08806. <https://doi.org/10.1029/2003GL018166>
- Coley, W. R., & Heelis, R. A. (1995). Adaptive identification and characterization of polar ionization patches. *Journal of Geophysical Research*, *100*(A12), 23,819–23,827. <https://doi.org/10.1029/95JA02700>
- Crowley, G. (1996). A critical review of ionospheric patches and blobs. In *Review of Radio Science 1993–1996* (pp. 619–648). New York: Oxford University Press.
- Foster, J. C., Coster, A. J., Erickson, P. J., Holt, J. M., Lind, F. D., Rideout, W., et al. (2005). Multiradar observations of the polar tongue of ionization. *Journal of Geophysical Research*, *110*, A09S31. <https://doi.org/10.1029/2004JA010928>
- Horwitz, J. L., & Lockwood, M. (1985). The cleft ion fountain: A two-dimensional kinetic model. *Journal of Geophysical Research*, *90*(A10), 9749–9762. <https://doi.org/10.1029/JA090iA10p09749>
- Iijima, T., & Potemra, T. A. (1976). Field-aligned currents in the dayside cusp observed by triad. *Journal of Geophysical Research*, *81*(34), 5971–5979. <https://doi.org/10.1029/JA081i034p05971>
- Kitamura, N., Ogawa, Y., Nishimura, Y., Terada, N., Ono, T., Shinbori, A., et al. (2011). Solar zenith angle dependence of plasma density and temperature in the polar cap ionosphere and low-altitude magnetosphere during geomagnetically quiet periods at solar maximum. *Journal of Geophysical Research*, *116*, A08227. <https://doi.org/10.1029/2011JA016631>
- Lockwood, M., & Carlson, H. C. (1992). Production of polar cap electron density patches by transient magnetopause reconnection. *Geophysical Research Letters*, *19*(17), 1731–1734. <https://doi.org/10.1029/92GL01993>
- Lockwood, M., Davies, J. A., Moen, J., van Eyken, A. P., Oksavik, K., McCrea, I. W., & Lester, M. (2005). Motion of the dayside polar cap boundary during substorm cycles: II. Generation of poleward-moving events and polar cap patches by pulses in the magnetopause reconnection rate. *Annales de Geophysique*, *23*(11), 3513–3532. <https://doi.org/10.5194/angeo-23-3513-2005>
- Ma, Y.-Z., Zhang, Q.-H., Xing, Z.-Y., Jayachandran, P. T., Moen, J., Heelis, R. A., & Wang, Y. (2018). Combined contribution of solar illumination, solar activity, and convection to ion upflow above the polar cap. *Journal of Geophysical Research*, *123*, 4317–4328. <https://doi.org/10.1029/2017JA024974>
- MacDougall, J., & Jayachandran, P. T. (2007). Polar patches: Auroral zone precipitation effects. *Journal of Geophysical Research*, *112*, A05312. <https://doi.org/10.1029/2006JA011930>
- Millward, C. H., Moffett, R. J., Balmforth, H. F., & Rodger, A. S. (1999). Modeling the ionospheric effects of ion and electron precipitation in the cusp. *Journal of Geophysical Research*, *104*(A11), 24,603–24,612. <https://doi.org/10.1029/1999JA000249>
- Oksavik, K., Ruohoniemi, J. M., Greenwald, R. A., Baker, J. B. H., Moen, J., Carlson, H. C., et al. (2006). Observations of isolated polar cap patches by the European incoherent scatter (EISCAT) Svalbard and super dual Auroral radar network (SuperDARN) Finland radars. *Journal of Geophysical Research*, *111*, A05310. <https://doi.org/10.1029/2005JA011400>
- Oksavik, K., van der Meeren, C., Lorentzen, D. A., Baddeley, L. J., & Moen, J. (2015). Scintillation and loss of signal lock from poleward moving auroral forms in the cusp ionosphere. *Journal of Geophysical Research: Space Physics*, *120*, 9161–9175. <https://doi.org/10.1002/2015JA021528>
- Rodger, A. S., Pinnock, M., Dudeney, J. R., Baker, K. B., & Greenwald, R. A. (1994). A new mechanism for polar patch formation. *Journal of Geophysical Research*, *99*(A4), 6425–6436. <https://doi.org/10.1029/93JA01501>
- Skjæveland, Å., Moen, J., & Carlson, H. C. (2011). On the relationship between flux transfer events, temperature enhancements and ion upflow events in the cusp ionosphere. *Journal of Geophysical Research*, *116*, A10305. <https://doi.org/10.1029/2011JA016480>
- Skjæveland, Å., Moen, J. I., & Carlson, H. C. (2014). Which cusp upflow events can possibly turn into outflows? *Journal of Geophysical Research: Space Physics*, *119*, 6876–6890. <https://doi.org/10.1002/2013JA019495>
- Strangeway, R. J., Ergun, R. E., Su, Y. J., Carlson, C. W., & Elphic, R. C. (2005). Factors controlling ionospheric outflows as observed at intermediate altitudes. *Journal of Geophysical Research*, *110*, A03221. <https://doi.org/10.1029/2004JA010829>
- Valladares, C. E., Decker, D. T., Sheehan, R., Anderson, D. N., Bullett, T., & Reinisch, B. W. (1998). Formation of polar cap patches associated with north-to-south transitions of the interplanetary magnetic field. *Journal of Geophysical Research*, *103*(A7), 14,657–14,670. <https://doi.org/10.1029/97JA03682>
- Wang, B., Nishimura, Y., Lyons, L. R., Zou, Y., Carlson, H. C., Frey, H. U., & Mende, S. B. (2016). Analysis of close conjunctions between dayside polar cap airglow patches and flow channels by all-sky imager and DMSP. *Earth, Planets and Space*, *68*(1), 150. <https://doi.org/10.1186/s40623-016-0524-z>
- Weber, E. J., Buchau, J. J., Moore, J. G., Sharber, J. R., Livingston, R. C., Winningham, J. D., & Reinisch, B. W. (1984). F layer ionization patches in the polar cap. *Journal of Geophysical Research*, *89*(A3), 1683–1694. <https://doi.org/10.1029/JA089iA03p01683>
- Zhang, Q.-H., Lockwood, M., Foster, J. C., Zhang, S.-R., Zhang, B.-C., McCrea, I. W., et al. (2015). Direct observations of the full Dungey convection cycle in the polar ionosphere for southward interplanetary magnetic field conditions. *Journal of Geophysical Research: Space Physics*, *120*, 4519–4530. <https://doi.org/10.1002/2015JA021172>
- Zhang, Q.-H., Ma, Y. Z., Jayachandran, P. T., Moen, J., Lockwood, M., Zhang, Y. L., et al. (2017). Polar cap hot patches: Enhanced density structures different from the classical patches in the ionosphere. *Geophysical Research Letters*, *44*, 8159–8167. <https://doi.org/10.1002/2017GL073439>
- Zhang, Q.-H., Zhang, B. C., Liu, R. Y., Dunlop, M. W., Lockwood, M., Moen, J., et al. (2011). On the importance of interplanetary magnetic field |by| on polar cap patch formation. *Journal of Geophysical Research*, *116*, A05308. <https://doi.org/10.1029/2010JA016287>
- Zhang, Q.-H., Zhang, B. C., Lockwood, M., Hu, H. Q., Moen, J., Ruohoniemi, J. M., et al. (2013). Direct observations of the evolution of polar cap ionization patches. *Science*, *339*(6127), 1597–1600. <https://doi.org/10.1126/science.1231487>
- Zhang, Q.-H., Zhang, B. C., Moen, J., Lockwood, M., McCrea, I. W., Yang, H. G., et al. (2013). Polar cap patch segmentation of the tongue of ionization in the morning convection cell. *Geophysical Research Letters*, *40*, 2918–2922. <https://doi.org/10.1002/grl.50616>
- Zhang, Q.-H., Zong, Q.-G., Lockwood, M., Heelis, R. A., Hairston, M., Liang, J., et al. (2016). Earth's ion upflow associated with polar cap patches: Global and in situ observations. *Geophysical Research Letters*, *43*, 1845–1853. <https://doi.org/10.1002/2016GL067897>
- Zou, Y., Nishimura, Y., Burchill, J. K., Knudsen, D. J., Lyons, L. R., Shiokawa, K., et al. (2016). Localized field-aligned currents in the polar cap associated with airglow patches. *Journal of Geophysical Research: Space Physics*, *121*, 10,172–10,189. <https://doi.org/10.1002/2016JA022665>

- Zou, Y., Nishimura, Y., Lyons, L. R., & Shiokawa, K. (2017). Localized polar cap precipitation in association with nonstorm time airglow patches. *Geophysical Research Letters*, *44*, 609–617. <https://doi.org/10.1002/2016GL071168>
- Zou, Y., Nishimura, Y., Lyons, L. R., Shiokawa, K., Donovan, E. F., Ruohoniemi, J. M., et al. (2015). Localized polar cap flow enhancement tracing using airglow patches: Statistical properties, IMF dependence, and contribution to polar cap convection. *Journal of Geophysical Research: Space Physics*, *120*, 4064–4078. <https://doi.org/10.1002/2014JA020946>